Ecohydrology & Hydrobiology 25 (2025) 42–53

Contents lists available at ScienceDirect

Ecohydrology & Hydrobiology

journal homepage: www.elsevier.com/locate/ecohyd

Original Research Article

Biogeochemical and microbial community structure differently modulates CO_2 and CH_4 dynamics in two adjacent volcanic lakes (Monticchio, Italy)

Stefano Fazi [a,*], Jacopo Cabassi [b], Francesco Capecchiacci [b,c,d], Cristiana Callieri [e], Ester M Eckert [e], Stefano Amalfitano [a], Luca Pasquini [f], Roberto Bertoni [e], Orlando Vaselli [b,c,g], Franco Tassi [b,c,h], Bertram Boehrer [i], Giovannella Pecoraino [j], Lorenza Li Vigni [j,k], Sergio Calabrese [j,k], Monia Procesi [h], Michele Paternoster [j,l]

[a] Water Research Institute, National Research Council (IRSA-CNR), Via Salaria 29.300, Monterotondo, Rome 00015, Italy
[b] Institute of Geosciences and Earth Resources, National Research Council (IGG-CNR), Via G. La Pira 4, Florence 50121, Italy
[c] Department of Earth Sciences, University of Florence, Via G. La Pira 4, Florence 50121, Italy
[d] Istituto Nazionale di Geofisica e Vulcanologia, Sezione di Napoli, Via Diocleziano 328, Napoli 80122, Italy
[e] Water Research Institute, National Research Council (IRSA-CNR), Molecular Ecology Group (MEG), Largo Tonolli 50, Verbania 28922, Italy
[f] Istituto Superiore di Sanità (ISS), Core Facilities, Viale Regina Elena 299, Rome 00161, Italy
[g] Istituto Nazionale di Geofisica e Vulcanologia, Sezione di Bologna, Viale Berti Pichat 6/2, Bologna 40127, Italy
[h] Istituto Nazionale di Geofisica e Vulcanologia, Sezione di Roma1, Via di Vigna Murata 605, Rome 00143, Italy
[i] Helmholtz Centre for Environmental Research (UFZ), Department Lake Research, Brueckstrasse 3a, Magdeburg 39114, Germany
[j] Istituto Nazionale di Geofisica e Vulcanologia, Sezione di Palermo, Via Ugo La Malfa 153, Palermo 90146, Italy
[k] Dipartimento di Scienze della Terra e del Mare (DiSTeM), University of Palermo, Via Archirafi 36, Palermo 90123, Italy
[l] Department of Sciences, University of Basilicata, Viale dell'Ateneo10, Potenza 85100, Italy

ARTICLE INFO

Keywords:
Carbon flux
Water chemistry
Dissolved gases
Methane
Cyanobacteria
Bacteria
Archaea

ABSTRACT

By hosting significant amounts of extra-atmospheric dissolved gases, including geogenic CO_2 and CH_4, volcanic lakes provide relevant ecosystem services through the key role the aquatic microbial community in mediating freshwater carbon fluxes. In view of elucidating the mechanisms governing the microbial spatial distribution and the possible implications for ecosystem functioning, we compared the hydrogeochemical features and the microbial community structure of two adjacent stratified volcanic lakes (Lake Grande - LG and Lake Piccolo - LP). Water chemistry, gases and their isotopic composition were coupled with microbial pigment profiling, cell counting, and phylogenetic analyses. LP showed transparent waters with low concentrations of chlorophyll-*a* and the occurrence of phycoerytrin-rich cyanobacteria. LG was relatively more eutrophic with a higher occurrence of diatoms and phycocyanine-rich cyanobacteria. Considering the higher concentrations of CO_2 and CH_4 in bottom waters, the oligotrophic LP was likely a more efficient sink of geogenic CO_2 in comparison to the adjacent eutrophic LG. The prokaryotic community was dominated by the mixothrophic hgcI clade (family Sporichthyaceae) in the LG surface waters, while in LP this taxon was dominant down to -15 m. Moreover, in LP, the bottom dark waters harbored a unique strictly anaerobic bacterial assemblage associated with methanogenic Archaea (i.e. Methanomicrobiales), resulting in a high biogenic methane concentration. Water layering and light penetration were confirmed as major factors affecting the microbial distribution patterns. The observed differences in the geochemical and trophic conditions reflected the structure of the aquatic microbial community, with direct consequences on the dynamics of dissolved greenhouse gases.

1. Introduction

Hundreds of volcanic lakes have been recorded and ascribed as a common feature in active and quiescent volcanic systems across the globe (interactive database VOLADA, Rouwet et al., 2021). Morphologies, watershed, dominant rock types, hydrogeological features of volcanic lakes are remarkably variable and reflect the worldwide geographical distribution of volcanic regions. In volcanic lakes,

* Corresponding author.
E-mail address: stefano.fazi@irsa.cnr.it (S. Fazi).

https://doi.org/10.1016/j.ecohyd.2023.12.003
Received 20 October 2023; Received in revised form 18 December 2023; Accepted 21 December 2023
Available online 18 January 2024

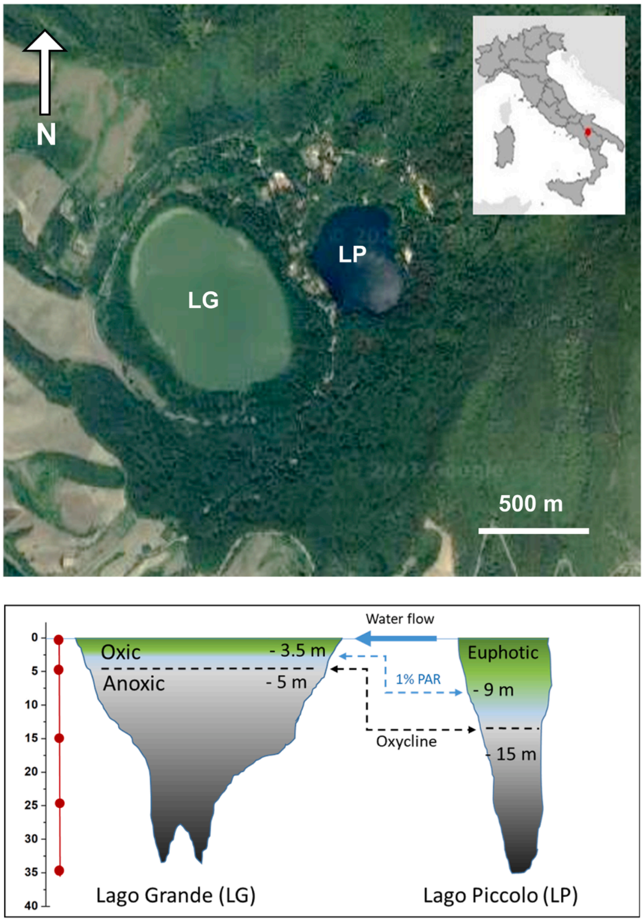

Fig. 1. Location of the two adjacent Monticchio Lakes, Lake Grande (LG) and Lake Piccolo (LP), and a schematic representation of the water stratification at the time of sampling. Red dots represent sampling points for microbial community characterization.

particularly those characterized by a permanent thermal and chemical stratification, external inputs of CO_2-rich hydrothermal gases may affect carbon budget at different extent (Tassi et al., 2018a; Cabassi et al., 2019). Moreover, the available water quality data, while limited, clearly indicated that trophic state can range consistently, from ultra-oligotrophic to highly eutrophic conditions, without any obvious major influence from the nearby volcanism (Larson, 1989). Long-termed studies on eutrophication of volcanic lentic systems showed that external carbon and nutrient inputs can accelerate all major biogeochemical cycles and promote specific microbial community interactions (Adamovich et al., 2019; Wang et al., 2023).

The lake trophic state is also a crucial factor in regulating CO_2 and methane dynamics (Beaulieu et al., 2019). The balance between heterotrophic processes, involving the microbial degradation of organic matter through respiration, and autotrophic processes, driven by phytoplankton and chemoautotrophs under light and dark conditions, can directly influence the overall CO_2 dynamics. Moreover, methane production can lead to CO_2 consumption, favoring gas development and storage at lake bottom (Schoell et al., 1988; Tassi et al., 2009; Boehrer et al., 2019; Bärenbold et al., 2020), while methane consumption can contribute to CO_2 production at either oxic (Bastviken et al., 2008; Savvichev et al., 2020) or anoxic conditions (e.g., sulfate-dependent anaerobic oxidation) (Knittel and Boetius 2009). Notably, a positive correlation between chlorophyll-*a* and methane levels was found in oxic lake waters and methanogenic microorganisms were recurrently detected in association with phytoplankton in oxygenated epilimnion and under saturated oxic conditions (Bizic et al. 2020; Fazi et al., 2021). As a result, given the different solubility of CO_2 and CH_4, biological processes can concurrently influence water density and lake vertical stratification by controlling the concentration ratio between the two gases (Koschorreck et al., 2008; Oswald et al., 2016; Cabassi et al., 2019; Tassi et al., 2018a).

Knowledge gaps currently persist on the role of volcanic lakes as sink or source of dissolved greenhouse gases and, more specifically, on the interplays between biogeochemical and microbial processes determining the fate of geogenic gas inputs. Moreover, only few studies emphasized the key role of microbially-mediated processes in modulating the natural gas dynamics in volcanic lakes (Löhr et al., 2006; Cabassi et al., 2014; Tiodjio et al., 2014, 2016; Mapelli et al., 2015; Tassi et al., 2018a).

By coupling the characteristics of water and dissolved gases to prokaryotic diversity in two adjacent lakes with different trophic conditions, i.e. the Monticchio lakes (hereafter named Lake Grande - LG, and Lake Piccolo - LP), the aims of this study were to (i) identify the key microbial players along the water column, and (ii) unveil the microbially-driven processes controlling the water and dissolved gas chemistry. We hypothesized that the water layering will affect the biogeochemical and microbial vertical profiles, with direct consequences on the overall carbon fluxes and dissolved greenhouse gas dynamics.

2. Methods

2.1. Sampling procedures and field measurements

LG and LP are maar lakes located on the SW flank of Mt. Vulture volcano (Monticchio, Basilicata, southern Italy). Previous studies (e.g., Cioni et al., 2006; Caracausi et al., 2013a) reported that while LP is a meromictic lake, LG is a warm monomictic lake displaying winter complete water turnover and spring new chemical stratification. In-depth and structured limnological studies were conducted in recent years (Spicciarelli and Marchetto 2019).

A multidisciplinary study campaign was carried out at the Monticchio lakes on June 27–28, 2018. LG and LP, located on the SW flank of Mt. Vulture volcano (Lat. 40,930,600°; Lon. 15,605,119°; Altitude 655 m a.s.l.), are characterized by surface areas of 4.1 and 1.6 $\times 10^5$ m^2 and maximum depths of 35 and 38 m, respectively (Fig. 1). LG has a prevalently flat bottom of about 12 m depth, with the maximum depth reached only in a narrow area in the NW sector of the basin, whereas LP has a regular bowl shape, characterized by steep walls and a flat central area (Caracausi et al., 2009; Cabassi et al., 2013). An artificial channel connects LP to LG, the latter having an outlet that discharges in the Ofanto river (Cioni et al., al. 2006; Schettler and Alberic 2008; Caracausi et al., 2013a). It is worth mentioning that according to Nicolosi (2010) and Caracausi et al. (2013a) both lakes receive groundwater inputs from the bottom.

Vertical profiles of temperature, electrical conductivity, pH, dissolved oxygen, turbidity, chlorophyll-*a* fluorescence excited on three wavelengths (at 470 nm, 530 nm, 610 nm; TRILUX sensor from Chelsea Technologies Ltd., UK) were measured at high resolution and accuracy at the deepest locations of each lake using a multiparameter probe (CTM90, Sea and Sun Technology, Germany). The vertical profiles of light intensity were measured throughout the water column at half a meter interval, using a light meter (LI-COR LI-250) with a submersible sensor for Photosynthetically Active Radiation (PAR, 400–700 nm), from a few centimeters below the water surface to the bottom. Secchi depth (m) was also measured in both lakes. Water and dissolved gas sampling was carried out at selected depths along the vertical profiles (LG: 0.5, 4, 5, 6, 15, 20, 25, 30 m and bottom; LP: 0.5, 2, 5, 8, 10, 15, 20, 25, 30 m and bottom), using the sampling method and equipment described in Tassi et al. (2004, 2009), Tassi and Rouwet (2014), and Cabassi et al. (2013, 2014). In particular, the single hose method, consisting of a Rilsan© tube with a diameter of 6 mm, lowered at the sampling depth, and connected to a 100 mL syringe equipped with a three-way PTFE valve, was used to pump the water at the surface after the displacement of a water volume at least twice the hose inner volume.

At each depth, one unfiltered and two filtered-acidified (0.45 μm, with ultrapure HCl and HNO_3, respectively) water samples were collected in polyethylene bottles for the analysis of anions (HCO_3^-, Cl^-, SO_4^{2-}, PO_4^{3-}, NO_3^-, Br^- and F^-), cations (Na^+, K^+, Ca^{2+}, Mg^{2+} and NH_4^+) and, at selected depths, Fe and Mn, respectively. Dissolved gases were sampled into one-way, pre-evacuated 250 mL glass vials equipped with a PTFE stopcock and used for the determination of the main gas chemical and isotopic (carbon expressed as $\delta^{13}C\text{-}CO_2$ and $\delta^{13}C\text{-}CH_4$ values) composition. The stopcock was opened to allow water entering into the vial (3/4 filled) once it was connected to the Rilsan© tube through the three-way valve (Tassi et al., 2009). Total Organic Carbon (TOC) concentration was measured with a total organic carbon analyzer (Shimadzu, 5000A). Five analyses were performed for each sample.

2.2. Chemical and isotopic analyses of water and dissolved gas samples

The chemical composition of water samples was determined by: i) automatic titration (analytical error <5 %) for HCO_3^- by using a Metrohm 794 automatic titration unit with 0.01 N HCl; ii) ion chromatography (analytical error <5 %) for the main anions and cations by using Metrohm 761 and Metrohm 861 chromatographs, respectively; iii) inductively coupled plasma mass spectrometry (ICP-MS, analytical error <10 %) for Fe and Mn contents by using an Agilent 7500-ce (e.g. Cabassi et al., 2019; Procesi et al., 2020). Inorganic dissolved gases (CO_2, N_2, Ar, and H_2) were analyzed by gas chromatography with thermal conductivity detector (GC-TCD) by using a Shimadzu 15A equipped with a 5 m long stainless steel column packed with Porapak 80/100 mesh, whereas CH_4 was analyzed by gas chromatography with flame ionization detector (GC-FID) by using a Shimadzu 14A equipped with a 10 m long stainless steel column packed with Chromosorb PAW 80/100 mesh coated with 23 % SP 1700 (Vaselli et al., 2006; Tassi et al., 2018a). The analytical error for GC analysis was <5 %. The gas composition was calculated based on i) composition, pressure and volume of the gas phase in the headspace of the sampled glass vial, and ii) the water solubility coefficients of each gas compound (Whitfield 1978). By assuming the equilibrium in the sampling vials between the separated gas phase and the liquid, the number of moles of each gas species in the liquid ($n_{i,l}$) was calculated on the basis of those in the flask headspace ($n_{i,g}$) according to the Henry's law constants (Wilhelm et al., 1977), the total moles of each gas species in the water sample resulting from the sum of $n_{i,l}$ and $n_{i,g}$. The partial pressures of each gas species were then computed according to the ideal gas law based on the total mole values (Tassi et al., 2018a). The sum of the partial pressures of the various species determined the total pressure reported in Table 2 for each depth. The $\delta^{13}C\text{-}CO_2$ and $\delta^{13}C\text{-}CH_4$ (in ‰ V-PDB) values in the headspace of the sampling flask were obtained by using a Picarro G2201-i analyzer, based on cavity ring-down spectroscopy (CRDS) (Venturi et al., 2021; Fazi et al., 2021). The analytical accuracy was ±0.2‰ for $\delta^{13}C\text{-}CO_2$ and ±1.2‰ for $\delta^{13}C\text{-}CH_4$.

2.3. Chlorophyll-a and photosynthetic efficiency

In addition to the in situ measurements, the concentration of chlorophyll-*a* (Chl) was also calculated using the Phyto-PAM with the right reference spectra for 3 phytoplankton algal groups (green, blue and brown) and a Chl calibration standard. In PhytoPAM, the light pulses are generated by an array of light-emitting diodes (LED) featuring 4 different colors: blue (470 nm), green (520 nm), light red (645 nm) and dark red (665 nm). Photomultiplier detectors enable extremely sensitive fluorescence detection down to a concentration of 0.1 μg Chl L^{-1} as it can be found in natural surface waters.

Photosynthetic efficiency, specifically the effective quantum yield of photosystem II, was used as an indicator of phytoplankton physiological status. It indicates the amount of light energy that is passing through photosystem II and is used to drive photosynthesis, rather than lost as heat or fluorescence. We used a Phyto-PAM (Pulse Amplitude Modulated) fluorometer to assess the effective quantum yield of energy conversion at the reaction center of PSII using saturation pulses. The instrument used in this research was equipped with the Optical Unit ED 101US/MP, the phyto ML (25 measuring LED in the 4 wavelengths and 12 actinic LED 655 nm), and the phyto AL (37 actinic LED 655 nm) (Schreiber et al., 1986). The Phyto-PAM allows the assessment of the effective quantum yield of energy conversion at the reaction center of PSII using saturation pulses. In dark adapted samples, the fluorescence measured before the saturation pulse is F_0 and the maximal fluorescence measured after the pulse is F_m. The ratio of the maximum variable fluorescence ($F_v= F_m\text{-}F_0$) to the maximum yield (F_m) provides the measurement of the maximal quantum conversion efficiency of photosystem II (PSII) and is known as the F_v/ F_m ratio (Genty et al., 1989).

2.4. Epifluorescence microscopy and flow cytometry

Visual inspections were conducted on all samples by epifluorescence microscopy detecting both primary autofluorescence and DAPI-staining fluorescence signals (5′, 6-diamino-2-phenylindole, final concentration, 0.1 μg mL^{-1}). Black polycarbonate filters (Poretics, 0.2 μm pore size) were used to collect the microbial cells, which were then observed by a Zeiss Axioplan microscope equipped with an HBO 100 W lamp, a Neofluar 100 x objective 1.25 x additional magnification and filter sets for UV (G365, FT395, LP420), blue (BP450–490, FT510, LP520) and green light excitation (LP510–560, FT580, LP590).

For cell counting, water samples (2 mL) were fixed with filtered formaldehyde (1 % final concentration) and stored at 4 °C in the dark until the analysis (i.e., completed within one week from sampling). Fixed water samples were analyzed by using three instruments with specific characteristics and sensitivities to detect the widest possible range of microbial targets by following harmonized protocols and workflows (e.g., gate design strategies): Accuri C6 (Becton Dickinson, Oxford, UK), A50-micro (Apogee Flow System, UK), FACS Canto I (BD Biosciences, USA). When using the above described protocols for the first time and on different machines, the first step was to run a sample containing about 10^6 reference beads per ml (e.g., 1 μm YG Polysciences), then tuning the voltages needed for the beads to appear in the upper right corner of the output cytogram (analytical error <10 %).

The flow cytometer Accuri C6, equipped with a 20 mW 488 nm Solid State Blue Laser and a 14.7 mW 640 nm Diode Red Laser, was used to count pigmented phytoplanktonic microorganisms: phycoerytrin (PE) and phycocyanin (PC) rich picocyanobacteria, pico- and micro-eukaryotes. The light scattering signals (forward and side light scatter, FSC and SSC, respectively), orange fluorescence (FL2 channel = 585/40 nm), and red fluorescence (FL3 channel >670 nm and FL4 channel 675/25) were acquired and considered for cells identification and quantification (Callieri et al., 2016). All data were acquired at a pre-set flow rate of 35 μl min^{-1}, in order to keep the number of total events below 1000 per second. The BD Accuri C6 software (v. 1.0.264.21) was used for data processing and a fixed template with the same gating strategy was applied to allow direct comparison between samples.

The bench-top flow cytometer A50-micro, equipped with a solid-state laser set at 20 mV and tuned to an excitation wavelength of 488 nm, was used for the quantification of non-pigmented heterotrophic microorganisms (prokaryotes and nanoflagellates) and cell aggregates through staining with SYBR Green I (Life Technologies; 1:10,000 dilution, 10 min at room temperature) and following protocols described elsewhere (Vergine et al., 2020). The light scattering signals (forward and side scatters), the green (530/30 nm) and red (>610 nm) fluorescence were acquired for the characterization of different cell groups targets. The intensity of green fluorescence emitted by SYBR-positive cells allowed for the discrimination among prokaryotic subgroups exhibiting two different nucleic acid contents (cells with low NA content

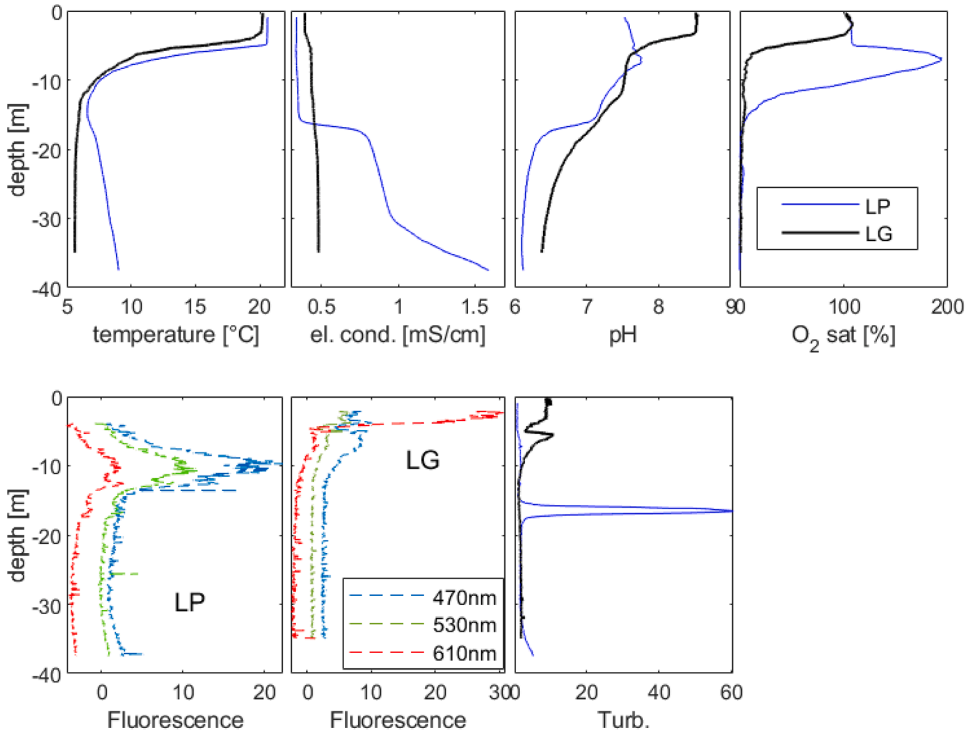

Fig. 2. Profiles of measured temperature, electrical conductivity (at 25 °C), pH and dissolved O_2 saturation, fluorescence of chlorophyll-*a* at three excitation wavelengths and turbidity. Lake Grande (LG) thick black lines and Lake Piccolo (LP) fine blue lines; Fluorescence measurements close to lake surfaces (1 to 2 m) could not be used.

- LNA; cells with high NA content – HNA, Amalfitano et al., 2018). The output data, plotted on a logarithmic scale over four fluorescence decades, were analyzed by the Apogee Histogram Software (v89.0). A threshold value was set on the green channel and samples were run at low flow rates to keep the number of events below 1000 events s^{-1}.

The lab-operating system FACS Canto I equipped with a 488-nm solid state laser with a 20-mW laser output was used for the quantification of virus-like particles (VLPs) according to the consolidated protocol described by Brussaard et al. (2010). Optical enhancements and a 4–3–3 configuration of fluorescence detectors (bands 530/30, 575/25, 695/40, 780/60 nm) provide high sensitivity and resolution for events with low intensities of scatter and fluorescence signals. The BD FACSCanto™ in-house software was used for setup, quality control, and data analysis.

2.5. High-throughput 16S rRNA amplicon sequencing and bioinformatics

For the microbial community analysis, 5 depths were sampled at LG and LP (0.5, 5, 15, 25 m and bottom). Lake water (1 L) was collected at each depth and immediately sub-aliquots were filtered with 0.2 µm pore-size polycarbonate filters (type GTTP; diameter, 47 mm; Millipore, Eschborn, Germany) and stored at −20 °C.

DNA was extracted from the filters by PowerSoil® DNA Isolation Kit (MoBio - Carlsbad, CA) according to the manufacturer's instructions. DNA was stored at −20 °C in small aliquots. Extracted DNA was amplified in a first PCR with the primer pairs 27F (5′-AGAGTTTGATCCTGGCTCAG-3′) and 534R (5′-ATTACCGCGGCTGCTGG-3′) and 340F (5′-CCCTAHGGGGYGCASCA-3) and 915R (5′-GWGCYCCCCCGYCAATTC-3′) targeting the regions V1-V3 and V3-V5 of bacterial and archaeal *16S rRNA* genes, respectively. All the generated raw reads were cleaned and clustered using the same pipeline for Bacteria and Archaea resulting in two OTU tables. Adaptors and primers were clipped from the sequences using cutadapt 1.9.1 (Martin 2011). The Usearch/Uparse pipeline was used for sequence assembly, quality filtration, chimera check and removal, and preparation of the database for the bacterial community composition (Edgar et al., 2011; Edgar 2013), mainly as suggested in the online tutorial with the following specifications: while merging, the max-diff parameter was set to 10, and then, sequences were filtered to a min-length of 376 and 450, for bacteria and archaea, respectively, with a max error of 0.5. The unnois3 command of UParse pipeline was used for the construction of zero radius operational taxonomic units (zOTUs; Edgar 2016). For the taxonomic assignments of zOTUs, the utax command was used with the Silva database version 123 (Quast et al., 2012) requiring a minimum similarity of 80 % for the taxonomic assignment. zOTUs assigned to non-bacterial taxa, such as chloroplasts (30 zOTUs or 0.7 % with 0.07 % of reads) and mitochondria (1 zOTU with 0.001 % of reads), were removed from the bacterial dataset, in the archaea dataset all were assigned to archaea.

All data analyses were conducted in R version 4.0.2 (R Core Team 2018), using package *ggplot2* (Wickham 2009) for graphical outputs, and package *reshape2* (Wickham 2012) for data preparation. For all statistical analyses, check of model assumptions and model fit were evaluated using package *performance* (Lüdecke et al., 2019). Samples were rarefied to 29,174 and 52,385 reads for bacteria and archaea, respectively, using the *GUniFrac* package (Chen et al., 2012). Richness was calculated as number of zOTUs per samples and plotted per basin and per depth for each lake basin. Generalized linear models assuming a *Poisson* distribution were made to test for the influence of sampling depth and basin (small, large lake basin) on Richness.

Beta-diversity was calculated as abundance based Bray-Curtis dissimilarity in the *vegan* package (Oksanen et al., 2007) and plotted as dendrogram using *hclust* with average linkage. To evaluate how basin and depth influence the Bray-Curtis dissimilarity we did a permutational analysis of variance (PERMANOVA) in the R package *vegan*. Mantel statistics was then used to evaluate the correlation between distances for bacteria and archaea. Taxonomy was plotted in stacked histograms both on a family and genus level. A correspondence analysis (CA) was used to visualize the degree of correspondence between sampling sites and prokaryotic families. All sequences are deposited in NCBI SRA with

Table 1
Temperature (°C), pH, chemical composition of the analyzed samples. Ion contents and Total Dissolved Solids (TDS) are in mg L^{-1}. Depth in meter. n.a.: not analyzed; n.d.: not detected. LG: Lake Grande; LP: Lake Piccolo. pH and temperature data were obtained from in-situ probe measurements.

Sample	Depth	Temperature	pH	HCO_3^-	F^-	Cl^-	Br^-	NO_3^-	SO_4^{2-}	PO_4^{3-}	Ca^{2+}	Mg^{2+}	Na^+	K^+	NH_4^+	Fe	Mn	TDS
LG1	0.5	20.2	8.5	195	1.3	28	0.09	2.8	13	n.d.	29	9.1	30	19	0.54	0.005	0.002	328
LG2	4	19.4	8.2	207	1.2	25	0.07	1.6	11	n.d.	32	9.4	30	18	0.56	n.a.	n.a.	337
LG3	5	15.9	7.7	210	1.2	28	0.10	1.8	12	n.d.	35	9.9	30	19	0.54	0.058	n.a.	347
LG4	6	11.4	7.6	219	1.3	28	0.09	4.1	12	n.d.	36	9.7	30	18	0.92	0.022	n.a.	359
LG5	10	7.2	7.5	217	1.3	27	0.11	4.9	11	n.d.	35	9.5	30	19	1.5	n.a.	n.a.	357
LG6	15	6.0	7.2	221	1.3	29	0.11	6.2	12	n.d.	36	9.8	31	18	1.7	n.a.	n.a.	364
LG7	20	5.7	6.8	246	1.1	24	0.05	0.12	9.3	0.13	37	11	31	20	2.3	n.a.	n.a.	381
LG8	25	5.6	6.6	256	0.93	20	0.11	9.9	8.0	0.27	39	12	30	19	3.7	0.55	n.a.	400
LG9	30	5.6	6.4	251	1.0	23	0.11	12	8.9	0.44	38	12	30	19	3.6	n.a.	n.a.	398
LG10	35	5.6	6.4	254	1.0	22	0.11	13	8.7	0.64	38	12	31	20	4.1	0.62	2.8	408
LP1	0.5	20.6	7.5	163	1.4	21	0.06	0.03	10	n.d.	21	5.8	29	19	0.64	0.011	0.004	272
LP2	2	20.6	7.6	166	1.2	18	0.05	0.08	8.6	n.d.	24	6.0	30	20	0.70	n.a.	n.a.	273
LP3	5	20.1	7.7	166	1.5	21	0.06	0.20	10	n.d.	22	5.7	29	18	0.60	n.a.	n.a.	275
LP4	8	9.7	7.7	163	1.2	17	0.06	0.65	8.2	n.d.	22	5.9	29	19	0.58	n.a.	n.a.	266
LP5	10	7.6	7.4	167	1.2	18	0.05	0.19	8.8	n.d.	26	5.8	29	20	0.64	n.a.	n.a.	275
LP6	15	6.6	7.2	177	1.5	21	0.08	0.46	9.5	n.d.	22	6.6	30	19	1.1	0.38	n.a.	288
LP7	20	7.5	6.3	488	1.3	22	0.28	0.05	2.3	n.d.	34	10	33	23	12	108	n.a.	733
LP8	25	7.9	6.2	493	1.0	21	0.23	0.09	2.7	0.09	35	10	34	24	14	123	n.a.	757
LP9	30	8.3	6.1	525	1.1	22	0.16	0.12	2.6	0.10	36	10	34	25	16	138	n.a.	810
LP10	37	9.0	6.1	920	0.97	19	0.59	0.06	2.1	0.14	45	12	36	27	40	275	2.3	1380

Table 2
Chemical composition (in mmol L^{-1}) of dissolved gases (CO_2, N_2, CH_4, Ar, O_2 and H_2), total pressure (in atm) and $\delta^{13}C$-CO_2 and $\delta^{13}C$-CH_4 (expressed as ‰ V-PDB) values of gas samples. Depth in meter. n.d.: not detected. LG: Lake Grande; LP: Lake Piccolo. O_2 data were obtained from in-situ probe measurements (see also Fig. 2).

Sample	Depth	CO_2	N_2	CH_4	Ar	O_2	H_2	pTOT	$\delta^{13}C$-CO_2	$\delta^{13}C$-CH_4
LG1	0.5	0.21	0.61	n.d.	0.014	0.29	n.d.	1.00	−8.6	−42.6
LG2	4	0.36	0.60	n.d.	0.015	0.24	n.d.	0.97	−8.0	−65.0
LG3	5	0.61	0.63	n.d.	0.014	0.12	n.d.	0.85	−8.6	−54.7
LG4	6	0.86	0.62	0.080	0.015	0.05	n.d.	0.81	−9.4	−45.2
LG5	10	1.23	0.61	0.13	0.014	n.d.	0.002	0.77	−7.4	−50.8
LG6	15	1.31	0.64	0.28	0.015	n.d.	0.004	0.86	−7.5	−52.3
LG7	20	2.67	0.62	0.44	0.015	n.d.	0.004	0.93	−7.4	−62.8
LG8	25	3.96	0.65	0.57	0.015	n.d.	0.008	1.04	−5.0	−58.5
LG9	30	4.21	0.66	0.69	0.016	n.d.	0.012	1.11	−5.5	−62.0
LG10	35	4.87	0.66	1.08	0.016	n.d.	0.014	1.30	−5.3	−61.3
LP1	0.5	0.11	0.62	n.d.	0.015	0.29	n.d.	1.04	−11.0	−52.0
LP2	2	0.19	0.63	n.d.	0.015	0.30	n.d.	1.04	−8.0	−51.7
LP3	5	0.27	0.61	n.d.	0.014	0.31	n.d.	0.96	−7.0	−29.0
LP4	8	0.33	0.63	n.d.	0.015	0.60	n.d.	0.91	−9.4	−36.2
LP5	10	0.95	0.61	0.011	0.015	0.42	n.d.	0.83	n.d.	n.d.
LP6	15	7.45	0.65	0.79	0.015	n.d.	0.004	1.21	−7.3	−52.7
LP7	20	10.23	0.64	1.54	0.015	n.d.	0.008	1.59	−2.6	−60.1
LP8	25	12.11	0.65	1.98	0.016	n.d.	0.011	1.83	−0.7	−59.8
LP9	30	13.34	0.66	2.45	0.016	n.d.	0.011	2.08	−2.4	−60.6
LP10	37	19.31	0.66	3.33	0.016	n.d.	0.015	2.59	1.6	−57.3

Accession Nr. PRJNA704791. Scripts and data are found on github (https://github.com/EsterME/Monticchio).

3. Results and discussion

3.1. Water geochemistry

Electrical conductivity (EC) of LG slightly increased with depth, while it showed a completely different vertical profile in LP by reaching 1.6 mS cm^{-1} at 36 m (Fig. 2). The water temperature in the epilimnion of both lakes was at about 21 °C and rapidly decreased to ~6 °C through the thermocline. While LG showed slightly decreasing temperatures for greater depths, LP showed a pronounced increase of temperatures below 15 m depth (to 9 °C above the lake bed), which was ascribed to a heat flow from the bottom into the lake waters (Caracausi et al., 2009). The vertical profile of the pH values at LG showed a decrease from the surface (~8.5) to 5 m depth (~7.6), followed by a less pronounced decreasing trend down to ~10 m depth and a more marked decrease down to the lake bottom (from ~7.5 to 6.3). The pH value at the surface of LP was about 7.5, followed by an increase (~7.8 at 7 m depth), a marked decrease down to ~15 m depth (~7.1) and a second decrease (from ~7.1 to 6.3) down to ~18 m depth. The dissolved oxygen in both lakes lay at 100 % saturation (about 10 mg L^{-1}) in the epilimnion. While LG showed an oxygen depletion through the thermocline and no oxygen in the deep water, LP showed a notable supersaturation in the thermocline reaching 200 % to drop to 0 for depths below 15 m.

The lakes showed relatively low Total Dissolved Solids (TDS) values and a $Ca^{2+}(Na^+)$-HCO_3^- composition (Table 1). The concentrations of $Ca^{2+}$and HCO_3^- significantly increased with depth (up to 45 and 920 mg L^{-1}, respectively, in LP), whereas those of SO_4^{2-} showed an opposite trend, ranging from 13 to 8.7 and from 10 to 2.1 mg L^{-1}, respectively, in LG and LP. The concentrations of the other main ionic compounds, i.e. Cl^- (up to 29 and 22 mg L^{-1}, respectively), Mg^{2+} (up to 12 mg L^{-1} in both lakes) and K^+ (up to 20 and 27 mg L^{-1}, respectively) did not show any significant vertical variation. Noteworthy, NH_4^+concentrations increased with depth of one order of magnitude in LG (from 0.54 to 4.1 mg L^{-1}) and two orders of magnitude in LP (from 0.64 to 40 mg L^{-1}). A similar trend was also shown by Fe and Mn, testifying the occurrence of anoxic conditions in the hypolimnion (Paternoster et al., 2016). It is worth to notice the very high concentrations of Fe (108–275 mg L^{-1}) in

Table 3
Values of the different parameters measured in the two Monticchio lakes: Lake Grande (LG) and Lake Piccolo (LP). TOC: Total Organic Carbon (mg L^{-1}), TN: total nitrogen (mg L^{-1}), Chl: chlorophyll-a (μg L^{-1}) measured by Phyto-PAM as total value and value of the different algal groups, F_v/F_m: photosynthetic efficiency (see methods). Depth in meter.

Sample	Depth	TOC	TN	Chl Blue	Chl Brown	Chl Tot	Fv/Fm blue	Fv/Fm brown
LG1	0.5	58.5	5.3	2.24	6.08	9.10	0.43	0.35
LG2	4	26.5	2.2	1.01	0.59	2.07	0.36	0.35
LG3	5	14.0	1.0	1.58	1.00	3.35	0.36	0.22
LG4	6	12.0	1.2	2.85	2.36	6.89	0.28	0.11
LG5	10	30.7	3.2	0.95	0.55	1.95	0.30	0.36
LG6	15	12.1	1.6	0.65	0.20	1.16	0.12	0.28
LG7	20	46.1	5.5	0.76	0.26	1.39	0.21	0.25
LG8	25	41.3	5.9	0.82	0.31	1.51	0.17	0.13
LG9	30	17.3	3.7	0.78	0.26	1.41	0.16	0.10
LG10	35	13.2	3.4	0.79	0.22	1.39	0.20	0.19
LP1	0.5	19.3	1.7	0.52	0.21	0.95	0.39	0.36
LP2	2	8.8	0.7	0.45	0.17	0.83	0.38	0.26
LP3	5	7.5	0.6	0.77	0.35	1.47	0.53	0.38
LP4	8	6.4	0.5	2.01	0.85	3.81	0.54	0.36
LP5	10	13.4	1.3	2.29	1.09	4.45	0.55	0.37
LP6	15	7.4	1.0	1.12	0.56	2.16	0.46	0.29
LP7	20	6.1	0.9	0.79	0.55	1.65	0.04	0.00
LP8	25	24.7	11.7	0.57	0.30	1.07	0.00	0.00
LP9	30	13.9	12.9	0.51	0.24	0.94	0.00	0.00
LP10	37	20.0	28.4	0.88	0.47	1.71	0.00	0.00

deepest waters of LP, likely related to contribution of CO_2-rich fluids, as testified by the gas emissions occurring along the shoreline of the lake (Martini et al., 1995). The concentrations of NO_3^- in LG and LP were relatively variable, i.e. from 0.12 to 13 and from 0.03 to 0.65 mg L^{-1}, respectively, with no clear trend with depth. PO_4^{3-}, Br^- and F^-contents were up to 0.64, 0.59 and 1.5 mg L^{-1}, respectively.

Overall, the chemical composition of Monticchio lakes, as that of volcanic lakes, is dependent on the balance between meteoric and hydrothermal fluids inputs (Tassi and Rouwet 2014). A meteoric origin, as reported in Cabassi et al. (2013), is consistent with the Ca^{2+}–HCO_3^- water composition of the two lakes (Table 1), which is typical for surface waters and shallow aquifers (Berner and Berner 1987). LG showed only weak salinity stratification and temperatures falling towards greater depths. On the contrary, LP showed a sharp gradient in electrical conductivity, rising temperatures in the monimolimnion towards the lake bottom balanced for density by the increase of dissolved substances and very high gas pressures. Such an accumulation usually requires a long period of stratification in which gases can accumulate (Horn et al., 2017; Boehrer et al., 2017; Boehrer et al., 2021).

3.2. Dissolved gases

Despite having different physical structures and dynamics (Caracausi et al., 2013a), both lakes are characterized by a hypolimnion and host a significant amount of extra-atmospheric dissolved gases, mostly consisting of CO_2 and CH_4 (Chiodini et al., 1997, 2000; Cioni et al., 2006; Zimmer et al., 2016). Our results showed that LP was characterized by a significant increase of dissolved gases with depth (up to 2.59 atm, in the range of that measured by Cabassi et al., 2013), whereas the vertical trend in LG was less evident (up to 1.30 atm). In both the lakes, N_2 dominates the dissolved gas composition of epilimnetic waters, whereas CO_2 was the most abundant species in the hypolimnion (up to 4.87 and 19.31 mmol L^{-1} at LG and LP, respectively), followed by CH_4 (up to 1.08 and 3.33 mmol L^{-1}, respectively). Deeper waters also showed increasing trends of H_2 (up to 0.014 and 0.015 mmol L^{-1}, respectively). Conversely, O_2 was rapidly decreasing along the vertical profiles down to 0 mmol L^{-1} below 6 and 14 m depths, respectively. The distribution along the vertical profile of Ar was not affected by substantial changes.

Hydrothermal inputs in the lakes are consistent with the highest CO_2 concentrations at the maximum depths (Table 2). HCO_3^- and pH reached respectively highest levels and lowest values at the maximum depths of the two lakes, being likely controlled by dissolved CO_2 (Cabassi et al., 2013). Nevertheless, the chemical and isotopic features of Monticchio lakes cannot exhaustively be explained by a mixing process between a meteoric and a hydrothermal source. The $\delta^{13}C$-CO_2 values at LG and LP ranged from −9.4 to −5.0 and from −11.0 to 1.6 ‰ V-PDB, respectively, whereas the $\delta^{13}C$-CH_4 values were comprised between −65.0 and −42.6 ‰ vs. V-PDB and between −60.6 and −29.0 ‰ vs. V-PDB, respectively. Such values are in the same range of that measured by Cabassi et al. (2013). The $\delta^{13}C$-CO_2 values (Table 2) at the lakes bottom were significantly less negative than those typically related to a pure organic source and to biogenic processes ($\delta^{13}C$-$CO_2 \leq -20$‰ vs. V-PDB; Faure 1986; Hoefs 2009) and in the range of those measured in the local fluid discharges (Caracausi et al., 2015), thus confirming the addition of extra-lacustrine carbon dioxide as generated by mixing of fluids

Table 4
Abundance of photosynthetic pigmented and heterotrophic non-pigmented microorganisms along the water column of Lake Grande (LG) and Lake Piccolo (LP). The occurrence of phycoerytrin (PE) and phycocyanin (PC) rich picocyanobacteria, microeukaryotes (Micro-EUK), prokaryotes (Prok), aggregates, heterotrophic nanoflagellates (HNF), and virus-like particles (VLPs) is expressed as cells or events per ml.

Sample	Depth m	PE-rich picocyano (10^3 cells/ml)	PC-rich picocyano (10^3 cells/ml)	Micro-EUK (10^3 cells/ml)	Prok (10^5 cells/ml)	LNA cells (% of Prok)	HNA cells (% of Prok)	Aggregates (10^4 evts/ml)	HNF (10^3 cells/ml)	VLPs 10^5 (evts/ml)
LG1	0.5	22.6	91.1	11.8	94.2	72.9	27.1	13.1	7.6	55.2
LG2	4	0.9	10.1	8.4	61.5	72.9	27.1	4.7	3.5	37.2
LG3	5	< 0.1	4.6	288.3	39.5	71.0	29.0	9.1	7.3	58.8
LG4	6	< 0.1	10.1	874.9	71.8	59.5	40.5	6.1	6.8	67.1
LG5	10	< 0.1	5.1	18.9	51.9	67.8	32.2	2.1	2.8	46.2
LG6	15	< 0.1	1.4	6.0	48.9	68.6	31.4	1.0	1.6	19.0
LG7	20	< 0.1	2.0	4.6	51.6	68.3	31.7	1.1	3.2	20.6
LG8	25	< 0.1	3.4	8.1	58.0	68.7	31.3	1.7	5.5	17.6
LG9	30	< 0.1	2.6	3.9	55.1	67.1	32.9	1.9	4.5	30.1
LG10	35	< 0.1	2.8	4.0	54.5	67.7	32.4	1.7	4.8	21.8
LP1	0.5	72.0	0.8	6.0	41.6	88.3	11.7	0.3	0.5	18.3
LP2	2	66.0	0.6	4.8	46.0	86.4	13.6	0.3	0.2	33.7
LP3	5	77.9	0.7	5.2	54.2	88.9	11.1	0.6	0.1	33.0
LP4	8	6.9	2.1	9.7	38.5	65.9	34.1	1.0	0.7	34.5
LP5	10	9.2	2.7	11.6	32.9	65.4	34.6	1.3	1.4	22.8
LP6	15	78.6	0.6	1.9	38.8	59.4	40.6	5.4	0.1	13.1
LP7	20	15.8	0.4	1.6	1.9	60.5	39.5	67.0	0.1	1.6
LP8	25	10.2	0.3	0.7	1.3	65.0	35.0	47.5	< 0.1	0.07
LP9	30	10.8	3.2	0.8	1.0	76.9	23.1	24.1	< 0.1	0.04
LP10	37	4.0	0.1	0.3	4.4	82.0	18.0	97.1	0.2	0.1

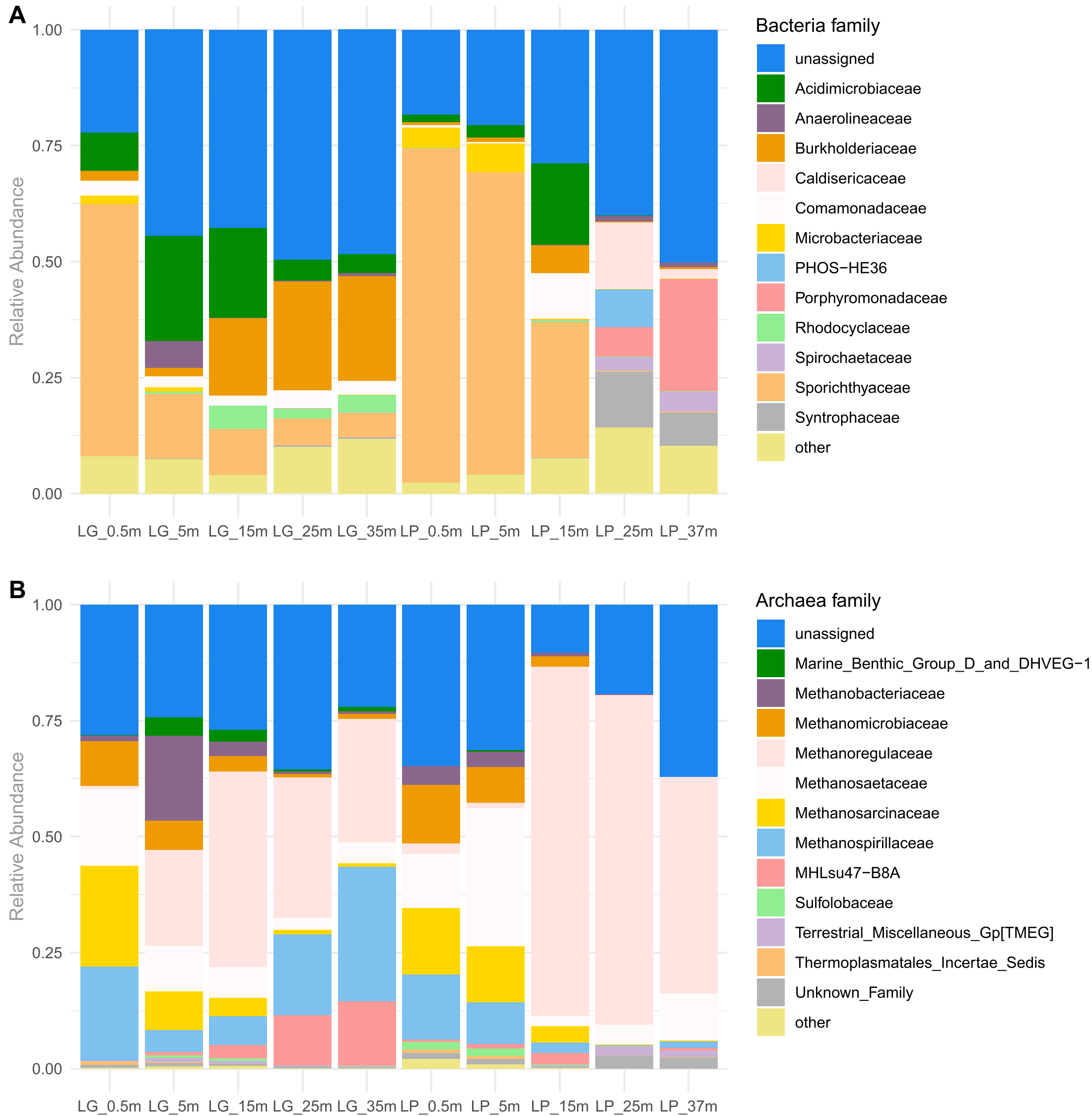

Fig. 3. Stacked bar chart of the relative abundances of A) bacterial and B) archael families in the samples from the sampled depths of Lake Grande (LG) and Lake Piccolo (LP). Families with less than 2000 and 1000 reads in the whole dataset for bacteria and archaea, respectively, were grouped in "others", zOTUs without any family assigned were grouped in "unassigned".

resulting from mantle and thermometamorphic reactions, the latter involving limestone (e.g. Minissale 2004). The negative trends of the $\delta^{13}C$-CO_2 values from the bottom to the surface of the lakes suggest that CO_2 partially originates from CH_4 oxidation occurring within the lake, especially in the relatively shallow, oxygenated water layers.

The high CH_4 concentrations and the strongly negative $\delta^{13}C$-CH_4 values (Table 2), significantly more negative than those typically produced by thermogenic processes (> −40‰ vs. V-PDB; Whiticar 1999), suggest biogenic CH_4 production, mostly occurring within bottom sediments and in the anaerobic deep waters (Schoell 1980, 1988). According to this hypothesis, the CH_4/CO_2 ratios are orders of magnitude higher than those measured in gases from bubbling pools located near the flanks of the Mt. Vulture (Caracausi et al., 2013b). It is also worth noting that the ^{13}C-enriched methane values of LP3 and LP4 samples are likely generated by oxidative processes, as already remarked by Cabassi et al. (2013). Overall, our results confirmed that methane is mainly produced by microbial activity, whilst CO_2 is both added to the lakes from sub-lacustrine hydrothermal vents and biogenically produced from CH_4 (Caracausi et al., 2009; Paternoster et al., 2016; Smith 2019). According to these features, these lakes can be classified as *bio-active* volcanic lakes (Cabassi et al., 2014). Rollover events, involving deep waters and followed by fish kill phenomena, have been reported in historical times (Caracausi et al., 2009).

3.3. Vertical profiles of the photoautotrophic community and chlorophyll

The chlorophyll data are a good proxy of phytoplankton biomass and give an indication of the prevalence of some algal groups in the two lakes. Our chlorophyll data from PhytoPAM show the dominance at LG surface layers of the brown algae corresponding to *Dinophyceae, Bacillariophyceae, Fragillariophyceae, Mediophyceae, Chrysophyceae* and to cyanobacteria at 6 m depth. LP has a lower Chl concentration with the maximum (4.54 μgL^{-1}) at 10 m depth, prevalently produced by blue-green algae (Table 3). Similar Chl values have been reported in a previous study on both lakes by satellite observations (Mancino et al., 2009).

The total organic carbon (TOC) concentrations ranged from 12 to 58 mg L^{-1} in LG and from 6 to 25 mg L^{-1} in LP, while the total Chl concentrations ranged from 1.16 to 9.1 μg L^{-1} at LG and from 0.83 to 4.4 μg L^{-1} at LP (Table 3). The rather high TOC concentration compared to the chlorophyll concentration, in the range of oligo and mesotrophic lakes, suggests that in both lakes the contribution of allochthonous TOC is

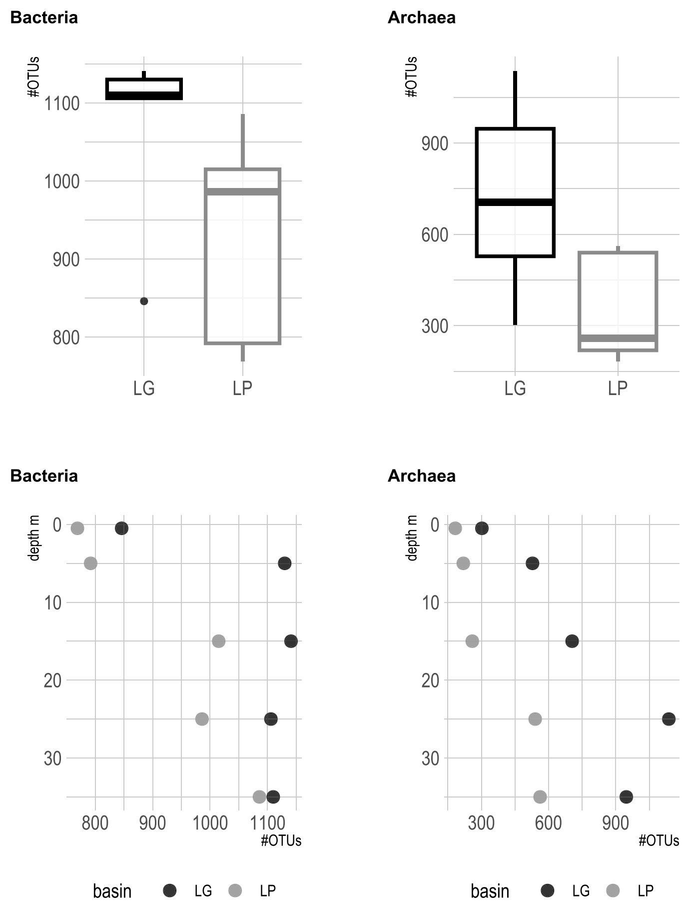

Fig. 4. Richness as numbers of zOTUs for bacteria and archaea in Lake Piccolo (LP) compared to Lake Grande (LG) (upper panels) and changes of richness with depth. Light gray dots refer to Lake Piccolo (LP) and dark gray ones to Lake Grande (LG).

significant in comparison to the autotrophic production of organic carbon.

The F_v/F_m ratio points to the presence of an efficient population of autotrophic cells in LP from 5 to 15 m depth, particularly of the cyanobacteria group. In LP, the ratio values abruptly dropped to zero down from 20 m depth and indicated the absence of photosynthetic activity in the deeper anoxic layers. In LG, there was a gradual decrease of the ratio values, indicating the possibility of photosynthetic activity even at depth with low light.

The most extensive study of phytoplankton communities was carried out in 2005 and 2006, especially at LG, while sporadic investigations were carried out at LP (Spicciarelli and Marchetto 2019). On the basis of the autotrophic communities occurring in the Monticchio lakes, LG waters were considered more eutrophic, with the presence of cyanobacterial populations dominated by *Microcystis aeruginosa, Woronichinia naegeliana*, and *Aphanocapsa delicatissima*. Conversely, LP was regarded as oligotrophic, with assemblages dominated by diatoms *Dinophyceae* and *Chlorophyceae* (Spicciarelli and Marchetto 2019). In previous studies, sampling was carried out on an annual base and did not consider the abundant picoautotrophic fraction mainly composed by cyanobacteria, as shown in this study.

The underwater irradiance (PAR) clearly indicates a difference in lake water transparency of the two lakes (Supplementary Figure 1), essentially confirming previous investigations that defined LG as eutrophic and LP as oligo-mesotrophic lakes (Spicciarelli and Marchetto 2019). The euphotic zone (i.e. the zone that extends from the surface to 1 % of the surface PAR) was 0÷3.5 m at LG and 0÷9 m at LP. Probe measurements imply that photosynthetic organisms are mainly present in the upper 4 m of the water column in LG, while in LP the fluorescence shows the strongest signal between 7 m and 12.5 m depth with a maximum at 10 m (Fig. 2). This agrees with the metalimnetic oxygen maximum at depths from 5 m to 10 m (maximum at 7 m) in LP and in the upper 4 m in LG. Fluorescence signals in all three excitation channels (at 470 nm, 510 nm and 610 nm) suggest the same species composition throughout the measured profile in LP. On the contrary, in LG only the excitation on the phycocyanin (610 nm) was very high near the surface, revealing a different phytoplankton composition in the two lakes. The turbidity peak in LP at 16 m depth was not directly connected to the presence of photosynthetic organisms.

The structure of the picophytoplanktonic community was very different between the two lakes. Picocyanobacteria of the genus *Synechococcus*, with phycoerytrin as dominant accessory pigment, are indeed prevalent at LP with a population of larger rod type cells peaking at 15 m depth and cocci dominating in the first 5 m (Table 4). The prevalence of phycoerytrin-rich picocyanobacteria at LP also supports the quality of the underwater light which is green-dominant (Callieri 1996; Callieri and Stockner 2002) and determines the prevalent accessory pigments in picocyanobacteria (Vörös et al., 1998; Stomp et al., 2007). Conversely, in LG, where the underwater light was red due to the many particles present in suspension, the prevalent picocyanobacteria are phycocyanin-rich types (Table 4). Similar results are also reported in the volcanic lakes from the Azores islands (Tassi et al., 2018b). In both LG and LP, the presence of picocyanobacteria in the deeper anoxic layers, even if in very low numbers, was observed. The survival of picocyanobacteria in such harsh conditions (depletion of light and oxygen) has recently been observed in one of the most important meromictic basin, i.e. the Black Sea, and with the isolated *Synechococcus* BS56D strain the potentials for alternative metabolisms to the photosynthetic fixation was demonstrated (Callieri et al., 2019; Di Cesare et al. 2020).

3.4. Vertical profiles of the heterotrophic microbiome

The abundance of planktonic prokaryotes, mostly represented by LNA cells, heterotrophic nanoflagellates, and virus-like particles decreased with depth in both lakes from the euphotic zone to the deeper water layers, as reported in most lentic systems (Berdjeb et al., 2011; Ram et al., 2019). At LG, values were similar throughout the water column (Prok = $5.9 \pm 1.5 \times 10^6$ cells mL^{-1}; HNF = $4.8 \pm 2.0 \times 10^3$ cells mL^{-1}; VLPs = $3.7 \pm 1.8 \times 10^6$ events mL^{-1}), with a nearly constant 1:2 virus-to-prokaryote ratio (VPR). At LP, vertical variations were found, with consistent changes in the anoxic deep waters. Prokaryotes and virus-like particles decreased consistently (Prok = $2.2 \pm 1.5 \times 10^5$ cells mL^{-1}; HNF = $0.4 \pm 0.4 \times 10^3$ cells mL^{-1}; VLPs = $0.5 \pm 0.8 \times 10^5$ events mL^{-1}) with VPR decreasing down to 1:5. Concurrently, the occurrence of microbial aggregates increased by one order of magnitude and reached the highest measured values ($5.9 \pm 3.1 \times 10^5$ events mL^{-1}) (Table 4). VPR values were in the lower range reported for freshwater systems and consistent with those from eutrophic and turbid environments in which a higher viral loss is expected (Parikka et al., 2017). The formation of microbial aggregates has been well documented in lakes and attributed to various abiotic and biotic factors (Grossart and Simon 1998; Amalfitano et al., 2017). Besides the direct exchange of metabolites through cell-to-cell interactions, cell proximity can offer further ecological advantages against adverse chemical conditions, size-dependent predation, and viral infection (Pernthaler 2005), possibly explaining the lower VPR values found in deep waters of LP.

Community profiles showed pronounced changes in taxonomic affiliation of the bacterial and archaeal communities, which were evident on both family or genus level (Fig. 3 and Supplementary Figure 2). Richness in terms of numbers of zOTUs after rarefaction showed very similar patterns for Bacteria and Archaea, namely significantly higher numbers of zOTU in LG compared to LP and a significant increase with depth in both lakes (Fig. 4, Supplementary Table S1). The

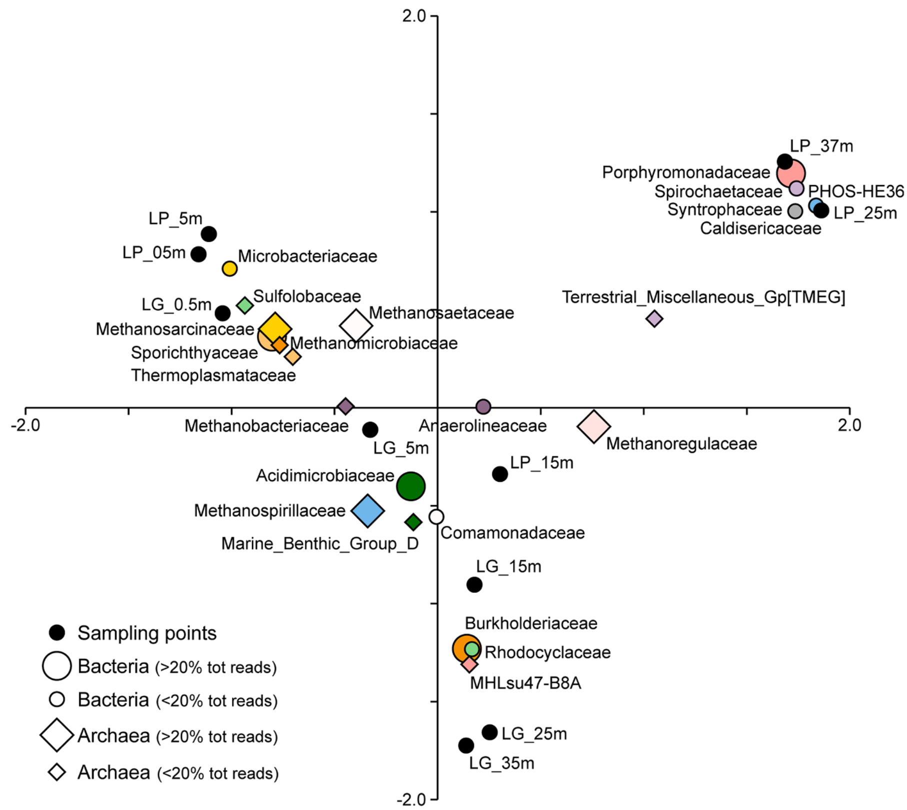

Fig. 5. Scatter plot calculated through the Correspondence Analysis (CA) of sampling sites and dominant prokaryotic taxa at the family level. Only families with more than 2000 and 1000 reads in the whole dataset, for bacteria and archaea respectively, were analyzed. The two CA axes representing most of the total inertia (i.e., with the highest eigenvalues) are shown.

bacterial and archaeal communities are highly correlated in terms of composition (Mantel test: $r = 0.9$, $p = 0.001$). Moreover, Alpha- and Beta-diversity measures denotes that the environmental conditions similarly affect the structuring of bacterial and archaeal communities in both lakes. This is not always the case, as in other habitats assembly patterns differ between the two domains (Ward et al., 2017; Wang et al., 2020; Hugoni et al., 2018). A larger fraction of variance is explained by the lake basin (Bacteria: R^2=0.28, $p = 0.001$. Archaea: R^2=0.29, $p = 0.001$. PERMANOVA). The lake with the higher trophic status (LG) harbored a microbial community with higher richness. Eutrophication may lead to changes in microbial community composition, affecting its functioning (Pizzetti et al., 2011). Recently, Kiersztyn et al. (2019) highlighted the dependence of the taxonomic composition on lake trophic state and suggested that eutrophication led to an increase in bacterial family richness and the evenness of their distribution. The prokaryotic communities were also significantly related to lake depth (Bacteria: R^2=0.22, $p = 0.008$. Archaea: R^2=0.19, $p = 0.02$. PERMANOVA), as shown in other volcanic lakes (Tassi et al., 2018a; Fazi et al., 2021).

Overall, it was possible to observe that surface oxic waters (i.e., LG_0.5 m, LP_0.5 m, LP_5 m) clustered together and showed a significantly different community composition than those found in deeper layers, with major differences clearly found in comparison to the bottom waters of LP (i.e., LP_25 m, LP_37 m) (Fig. 5, Supplementary Figure 3). In oxic waters, a pronounced dominance of the Actinobacteria family *Sporichthyaceae* (mainly represented by hgcI clade) was observed, along with the higher occurrence of archaeal Methanomicrobia of the families *Methanosarcinaceae and Methanosaetaceae* (mainly represented by the genera Methanosarcina, Methanomethylovorans and Methanosaeta). The hgcI clade is common and abundant in a wide range of freshwater habitats and reports to metabolize carbohydrate and N-rich organic compounds at either illuminated oxic or dark anoxic conditions (Warnecke et al., 2004; Ghylin et al., 2014; Liu et al., 2015). The retrieved archaeal genera were reported to be actively involved in methane production through the three metabolic pathways and notably found in the oxic surface waters at high levels of primary production (Fazi et al., 2021).

In deeper anoxic waters, the consistent shift in the prokaryotic community composition is related to the prompt increase of *Methanoregulaceae* (genus *Methanoregula*) in both lakes. In LP, the genus *Methanoregula* reached more than 75 % of total archaeal reads, whereas Archaea in LG were also consistently represented by the family *Methanospirillaceae* (genus *Methanospirillum*). Notably, the archaeal members retrieved in the anoxic waters of both lakes are strictly anaerobic and hydrogenotrophic methanogens (Garcia et al., 2006).

The bacterial communities in bottom waters were also remarkably different between LG and LP. In particular, the Betaproteobacteria families *Burkholderiaceae* and *Rhodocyclaceae*, along with the Actinobacteria of the family Acidimicrobiaceae, dominates in LG. The family *Burkholderiaceae* is mainly represented by the genus *Polynucleobacter*, a largely distributed member of bacterioplankton in freshwater systems (Newton et al., 2011). Among *Acidimicrobiaceae*, the genus CL500–29_marine_group, is reported to be associated with cyanobacteria (Yu et al., 2019). In the deeper layers of LP (LP_25 m and LP_37 m), the bacterial community is dominated by members of the family *Porphyromonadaceae*, mainly represented by the genus *Paludibacter*, known as fermentative bacteria transitorily shifting from microbial biofilm to suspended biomass (Zakaria et al., 2019). The families *Caldisericaceae*, PHOS-HE36, *Synthrophaceae*, and *Spirochaetaceae* are also relatively abundant in LP bottom waters. Notably, members of these families were reported as particle-associated anaerobic chemoorganotrophs (Cohen et al., 2021) that could find favorable syntrophic relations within the numerous microbial aggregates retrieved in LP bottom waters. Overall, the biogeochemical vertical profiles affected the phylogenetic composition and the interplay between bacterial and archaeal communities by opening niches for specialized microbial processes.

4. Conclusions

This study provides insights on the interplays between water chemistry, dissolved gases, carbon flux dynamics, and the aquatic microbial community along vertical profiles of the two adjacent lakes with different water mixing, stratification and trophic conditions. The differences in geochemical characteristics and light penetration shape the microbial community, directly affecting biogeochemical processes across the water column of the two adjacent lakes. The meromictic lake (LP) is a more efficient sink of geogenic CO_2 in comparison to the adjacent eutrophic monomictic lake (LG). Our results provides further evidence on the effects of water stratification and trophic conditions on the complexity of the microbial community, with direct implications on the dynamics of dissolved greenhouse gases. The outcomes of this study could contribute to better understand the feedback loops between freshwater eutrophication and GHG emission.

Compliance with ethical standards

The authors declare no conflicts of interests. The Research did not involve Human Participants and/or Animals.

Data availability

All sequences are deposited in NCBI SRA with Accession Nr. PRJNA704791. Scripts and data are found on github (https://github.com/EsterME/Monticchio). All other data (geochemical variables, abundance of microbial cells) are available from the corresponding author on reasonable request.

Author contribution

FT, JC, FC, SF, CC, RB, OV, BB, GP, SC, MPR, MPA contributed to conceptualization. All authors contributed to investigation,data curation, and formal analysis.. SF, SA, JC contributed to writing - original draft. All authors contributed to writing - review and editing.

Declaration of competing interest

We state that there are no conflicts of interest or any financial interest for all authors of the manuscript entitled “Biogeochemical and microbial community structure differently modulates CO2 and CH4 dynamics in two adjacent volcanic lakes (Monticchio, Italy)” by Stefano Fazi, Jacopo Cabassi, Francesco Capecchiacci, Cristiana Callieri, Ester M Eckert, Stefano Amalfitano, Luca Pasquini, Roberto Bertoni, Orlando Vaselli, Franco Tassi, Bertram Boehrer, Giovannella Pecoraino, Lorenza Li Vigni, Sergio Calabrese, Monia Procesi, Michele Paternoster.

Authors state that the research was conducted according to ethical standards.

Acknowledgments

The work is the result of the International Summer Meeting on Volcanic Lakes “Different perspectives and approaches to study a volcanic lake” held at Monticchio lakes (Basilicata, Italy) on June 2018. The sampling campaign was carried out by an international team during the meeting. The work largely benefited from the discussions among participants during this event. Authors wish to thank Lorenzo Pin, for valuable suggestions.

Supplementary materials

Supplementary material associated with this article can be found, in the online version, at doi:10.1016/j.ecohyd.2023.12.003.

References

Adamovich, B.V., Medvinsky, A.B., Nikitina, L.V., Radchikova, N.P., Mikheyeva, T.M., Kovalevskaya, R.Z., Zhukova, T.V., 2019. Relations between variations in the lake bacterioplankton abundance and the lake trophic state: evidence from the 20-year monitoring. Ecol. Indic. 97, 120–129.
Amalfitano, S., Corno, G., Eckert, E., Fazi, S., Ninio, S., Callieri, C., Grossart, H.P., Eckert, W., 2017. Tracing particulate matter and associated microorganisms in freshwaters. Hydrobiologia 800 (1), 145–154.
Amalfitano, S., Fazi, S., Ejarque, E., Freixa, A., Romaní, A.M., Butturini, A., 2018. Deconvolution model to resolve cytometric microbial community patterns in flowing waters. Cytometry Part A 93 (2), 194–200.
Bastviken, D., Cole, J.J., Pace, M.L., Van de Bogert, M.C., 2008. Fates of methane from different lake habitats: connecting whole-lake budgets and CH4 emissions. J. Geophys. Res. 113 (G2).
Bärenbold, F., Boehrer, B., Grilli, R., Mugisha, A., von Tümpling, W., Umutoni, A., Schmid, M., 2020. No increasing risk of a limnic eruption at Lake Kivu: intercomparison study reveals gas concentrations close to steady state. PLoS ONE 15 (8), e0237836.
Berdjeb, L., Pollet, T., Domaizon, I., Jacquet, S., 2011. Effect of grazers and viruses on bacterial community structure and production in two contrasting trophic lakes. BMC Microbiol. 11 (1), 1–18.
Berner, E.K., Berner, R.A., 1987. Global Water Cycle: Geochemistry and Environment. Prentice-Hall, Inc, Englewood Cliffs, New Jersey, p. 397.
Beaulieu, J.J., DelSontro, T., Downing, J.A., 2019. Eutrophication will increase methane emissions from lakes and impoundments during the 21st century. Nat. Commun. 10 (1), 1–5.
Bižić, M., Klintzsch, T., Ionescu, D., Hindiyeh, M.Y., Günthel, M., Muro-Pastor, A.M., Grossart, H.P., 2020. Aquatic and terrestrial cyanobacteria produce methane. Sci. Adv. 6 (3), eaax5343.
Boehrer, B., von Rohden, C., Schultze, M., 2017. Physical features of meromictic lakes: stratification and circulation. Ecology of Meromictic lakes. Springer, pp. 15–34.
Boehrer, B., von Tuempling, W., Mugisha, A., Rogemont, C., Umutoni, A., 2019. Reliable reference for the methane concentrations in Lake Kivu at the beginning of industrial exploitation. Hydrol. Earth Syst. Sci. 23 (11), 4707–4716.
Boehrer, B., Jordan, S., Leng, P., Waldemer, C., Schwenk, C., Hupfer, M., Schultze, M., 2021. Gas pressure dynamics in small and mid-size lakes. Water (Basel) 13 (13), 1824.
Brussaard, C.P.D., Payet, J.P., Winter, C., Weinbauer, M.G., 2010. Chapter 11: Quantification of Aquatic Viruses By Flow Cytometry Manual of Aquatic Viral Ecology. American Society of Limnology and Oceanography, Waco, TX. https://doi.org/10.4319/mave2010978-0-9845591-0-7.
Cabassi, J., Tassi, F., Vaselli, O., Fiebig, J., Nocentini, M., Capecchiacci, F., Rouwet, D., Bicocchi, G., 2013. Biogeochemical processes involving dissolved CO_2 and CH_4 at Albano, Averno, and Monticchio meromictic volcanic lakes (Central–Southern Italy). Bull. Volcanol. 75 (1), 1–19.
Cabassi, J., Tassi, F., Mapelli, F., Borin, S., Calabrese, S., Rouwet, D., Chiodini, G., Marasco, R., Chouaia, B., Avino, R., Vaselli, O., Pecoraino, G., Capecchiacci, F., Bicocchi, G., Caliro, S., Ramirez, C., Mora-Amador, R., 2014. Geosphere-biosphere interactions in bio-activity volcanic lakes: evidences from Hule and Rìo Cuarto (Costa Rica). PLoS ONE 9 (7), e102456. https://doi.org/10.1371/journal.pone.0102456.
Cabassi, J., Capecchiacci, F., Magi, F., Vaselli, O., Tassi, F., Montalvo, F., Caprai, A., 2019. Water and dissolved gas geochemistry at Coatepeque, Ilopango and Chanmico volcanic lakes (El Salvador, Central America). J. Volcanol. Geotherm. Res. 378, 1–15.
Callieri, C., 1996. Extinction coefficient of red, green and blue light and its influence on picocyanobacterial types in lakes at different trophic levels. Memorie dell'Istituto italiano di Idrobiologia 54, 35–142.
Callieri, C., Stockner, J.G., 2002. Freshwater autotrophic picoplankton: a review. J. Limnol. 61, 1–14.
Callieri, C., Amalfitano, S., Corno, G., Bertoni, R., 2016. Grazing-induced *Synechococcus* microcolony formation: experimental insights from two freshwater phylotypes. FEMS Microbiol. Ecol. 92, fiw154.
Callieri, C., Slabakova, V., Dzhembekova, N., et al., 2019. The mesopelagic anoxic Black Sea as an unexpected habitat for Synechococcus challenges our understanding of global “deep red fluorescence”. ISME J. 13 (7), 1676–1687.
Caracausi, A., Nuccio, P.M., Favara, R., Nicolosi, M., Paternoster, M., 2009. Gas hazard assessment at the Monticchio crater lakes of Mt Vulture, a volcano in Southern Italy. Terra Nova 21, 83–87.
Caracausi, A., Nicolosi, M., Nuccio, P.M., Favara, R., Paternoster, M., Rosciglione, A., 2013a. Geochemical insight into differences in the physical structures and dynamics of two adjacent maar lakes at Mt Vulture volcano (southern Italy). Geochem., Geophys., Geosyst. 14 (5), 1606–1625.

Caracausi, A., Martelli, M., Nuccio, P.M., Paternoster, M., Stuart, F.M., 2013b. Active degassing of mantle-derived fluid: a geochemical study along the Vulture line southern Apennines (Italy). J. Volcanol. Geotherm. Res. 253, 65–74.
Caracausi, A., Paternoster, M., Nuccio, P.M., 2015. Mantle CO_2 degassing at Mt Vulture volcano (Italy): relationship between CO_2 outgassing of volcanoes and the time of their last eruption. Earth Planet. Sci. Lett. 411, 268–280.
Chen, J., Bittinger, K., Charlson, E.S., et al., 2012. Associating microbiome composition with environmental covariates using generalized UniFrac distances. Bioinformatics 28, 2106–2113.
Chiodini, G., Cioni, R., Guidi, M., Marini, L., Principe, C., Raco, B., 1997. Water and gas chemistry of the Lake Piccolo of Monticchio (Mt Vulture, Italy). Curr. Res. Volcanic Lakes 10, 3–8.
Chiodini, G., Cioni, R., Guidi, M., Magro, G., Marini, L., Raco, B., 2000a. Gas chemistry of the Lake Piccolo of Monticchio, Mt Vulture, in December 1996. Acta Vulcanol. 12, 139–142.
Cohen, A.B., Klepac-Ceraj, V., Butler, K., Weber, F., Garber, A.I., Christensen, L.N., Cram, J.A., McCormick, M.L., Taylor, G.T., 2021. Particle-associated and free-living microbial assemblages are distinct in a permanently redox-stratified freshwater lake bioRxiv 2021.11.24.469905; https://doi.org/10.1101/2021.11.24.469905.
Cioni, R., Marini, L., Raco, B., 2006. The Lake Piccolo di Monticchio: fluid geochemistry and evaluation of the limnic eruption hazard. In: Principe, C (Ed.), The Geology of Mount Vulture. CNR, Regione Basilicata, pp. 171–177 ed.
Di Cesare, A., Dzhembekova, N., Cabello-Yeves, P.J., et al., 2020. Genomic comparison and spatial distribution of different *Synechococcus* phylotypes in the Black Sea. Front. Microbiol. 11, 1979.
Edgar, R.C., 2013. UPARSE: highly accurate OTU sequences from microbial amplicon reads. Nat. Methods 10, 996–998.
Edgar, R.C., 2016. UNOISE2: improved error-correction for Illumina 16S and ITS amplicon sequencing. Biorxiv, 081257.
Edgar, R.C., Haas, B.J., Clemente, J.C., Quince, C., Knight, R., 2011. UCHIME improves sensitivity and speed of chimera detection. Bioinformatics 27, 2194–2200.
Faure, G., 1986. Inorganic Geochemistry. Macmillan Pub Com, p. 627.
Fazi, S., Amalfitano, S., Venturi, S., et al., 2021. High concentrations of dissolved biogenic methane associated with cyanobacterial blooms in East African lake surface water. Commun. Biol. 4, 845. https://doi.org/10.1038/s42003-021-02365-x.
Garcia, J.L., Ollivier, B., Whitma, W.B., 2006. The Order Methanomicrobiales. In: Prokaryotes 3, 208–230.
Genty, B., Briantais, J.M., Baker, N.R., 1989. The relationship between the quantum yield of photosynthetic electron transport and quenching of chlorophyll fluorescence. Biochimica et Biophysica Acta (BBA)-General Subj. 990 (1), 87–92.
Ghylin, T.W., Garcia, S.L., Moya, F., Oyserman, B.O., Schwientek, P., Forest, K.T., McMahon, K.D., 2014. Comparative single-cell genomics reveals potential ecological niches for the freshwater acI Actinobacteria lineage. ISME J. 8 (12), 2503–2516.
Grossart, H.P., Simon, M., 1998. Significance of limnetic organic aggregates (lake snow) for the sinking flux of particulate organic matter in a large lake. Aquat. Microb. Ecol. 15 (2), 115–125.
Hoefs, J., 2009. Stable Isotope Geochemistry, 6th edn. Springer, Berlin, p. 288.
Horn, C., Metzler, P., Ullrich, K., Koschorreck, M., Boehrer, B., 2017. Methane storage and ebullition in monimolimnetic waters of polluted mine pit lake Vollert-Sued, Germany. Sci. Total Environ. 584, 1–10.
Hugoni, M., Escalas, A., Bernard, C., Nicolas, S., Jezequel, D., Vazzoler, F., Agogué, H., 2018. Spatiotemporal variations in microbial diversity across the three domains of life in a tropical thalassohaline lake (Dziani Dzaha, Mayotte Island). Mol. Ecol. 27 (23), 4775–4786.
Kiersztyn, B., Chróst, R., Kaliński, T., et al., 2019. Structural and functional microbial diversity along a eutrophication gradient of interconnected lakes undergoing anthropopressure. Sci. Rep. 9, 11144. https://doi.org/10.1038/s41598-019-47577-8.
Knittel, K., Boetius, A., 2009. Anaerobic oxidation of methane: progress with an unknown process. Annu. Rev. Microbiol. 63, 311–334.
Koschorreck, M., Wendt-Potthoff, K., Scharf, B., Richnow, H.H., 2008. Methanogenesis in the sediment of the acidic Lake Caviahue in Argentina. J. Volcanol. Geotherm. Res. 178, 197–204.
Larson, G.L., 1989. Geographical distribution, morphology and water quality of caldera lakes: a review. Hydrobiologia 171 (1), 23–32.
Liu, J., Fu, B., Yang, H., et al., 2015. Phylogenetic shifts of bacterioplankton community composition along the Pearl Estuary: the potential impact of hypoxia and nutrients. Front. Microbiol. 6, 64.
Löhr, A.J., Laverman, A.M., Braster, M., Van Straalen, N.M., Röling, W.F., 2006. Microbial communities in the world's largest acidic volcanic lake, Kawah Ijen in Indonesia, and in the Banyupahit River originating from it. Microb. Ecol. 52 (4), 609–618.
Lüdecke, D., Makowski, D., Waggoner, P., 2019. Performance: assessment of regression models performance. R package version 0.4. 2.
Mancino, G., Nolè, A., Urbano, V., Amato, M., Ferrara, A., 2009. Assessing water quality by remote sensing in small lakes: the case study of Monticchio lakes in Southern Italy. iForest-Biogeosci. Forestry 2 (4), 154.
Mapelli, F., Marasco, R., Rolli, E., Daffonchio, D., Donachie, S., Borin, S., 2015. Microbial life in volcanic lakes. Volcanic Lakes. Springer, Berlin, Heidelberg, pp. 507–522.
Martin, M., 2011. Cutadapt removes adapter sequences from high-throughput sequencing reads. EMBnet. J. 17 (1), 10–12.
Martini, M., Tassi, F., Giannini, L., Vaselli, O., 1995. Monticchio crater lakes (Italy): hazardous CO2 reservoir? Curr. Res. Volcanic Lakes 8, 11–17.
Minissale, A., 2004. Origin, transport and discharge of CO_2 in central Italy. Earth-Sci. Rev. 66, 89–141.
Newton, R.J., Jones, S.E., Eiler, A., McMahon, K.D., Bertilsson, S., 2011. A guide to the natural history of freshwater lake bacteria. Microbiol. Mol. Biol. Rev. 75, 14–49.
Nicolosi, M., 2010. The Monticchio crater lakes: fluid geochemistry and circulation dynamics. PhD Thesis, University of Palermo (Italy), p. 132.
Oksanen, J., Kindt, R., Legendre, P., et al., 2007. The vegan package. Commun. Ecol. Pack. 10 (631–637), 719.
Oswald, K., Milucka, J., Brand, A., et al., 2016. Aerobic gammaproteobacterial methanotrophs mitigate methane emissions from oxic and anoxic lake waters. Limnol. Oceanogr. 61, 101–118.
Parikka, K.J., Le Romancer, M., Wauters, N., Jacquet, S., 2017. Deciphering the virus-to-prokaryote ratio (VPR): insights into virus–host relationships in a variety of ecosystems. Biol. Rev. 92 (2), 1081–1100.
Paternoster, M., Mongelli, G., Caracausi, A., Favara, R., 2016. Depth influence on the distribution of chemical elements and saturation index of mineral phases in twins maar lakes: the case of the Monticchio lakes (Southern Italy). J. Geochem. Explor. 163, 10–18.
Pernthaler, J., 2005. Predation on prokaryotes in the water column and its ecological implications. Nat. Rev. Microbiol. 3 (7), 537–546.
Pizzetti, I., Gobet, A., Fuchs, B.M., Amann, R., Fazi, S., 2011. Abundance and diversity of Planctomycetes in a Tyrrhenian coastal system of central Italy. Aquat. Microb. Ecol. 65 (2), 129–141.
Procesi, M., Cinti, D., Casentini, B., Cabassi, J., Amalfitano, S., Pizzino, L., Fazi, S., 2020. Geochemical characterization of an urban lake in the centre of Rome (Lake Bullicante, Italy). Italian J. Geosci. 139 (3), 436–449.
Ram, A.S.P., Keshri, J., Sime-Ngando, T., 2019. Distribution patterns of bacterial communities and their potential link to variable viral lysis in temperate freshwater reservoirs. Aquat. Sci. 81 (4), 1–12.
Rouwet, D., Nemeth, K., Tamburello, G., Calabrese, S., Issa, 2021. Volcanic Lakes in Africa: the VOLADA_Africa 2.0 Database, and Implications for Volcanic Hazard. New Front. Rare Earth Sci. Appl., Proc. Int. Conf. Rare Earth Dev. Appl. 9, 717798 https://doi.org/10.3389/feart.2021.717798.
Quast, C., Pruesse, E., Yilmaz, P., et al., 2012. The SILVA ribosomal RNA gene database project: improved data processing and web-based tools. Nucleic Acids Res. 41, D590–D596.
Savvichev, A.S., Kadnikov, V.V., Rusanov, I.I., et al., 2020. Microbial processes and microbial communities in the water column of the polar meromictic Lake Bol'shie Khruslomeny at the White Sea coast. Front. Microbiol. 11, 1945.
Schettler, G., Alberic, P., 2008. Laghi di Monticchio (Southern Italy, Region Basilicata): genesis of sediments – a geochemical study. J. Paleolimnol. 40, 529–556.
Schoell, M., 1980. The hydrogen and carbon isotopic composition of methane from natural gases of various origins. Geochim. Cosmochim. Acta 44, 649–661.
Schoell, M., Tietze, K., Schoberth, S., 1988. Origin of the methane in Lake Kivu (east-central Africa). Chem. Geol. 71, 257–265.
Schreiber, U., Schliwa, U., Bilger, W., 1986. Continuous recording of photochemical and non-photochemical chlorophyll fluorescence quenching with a new type of modulation fluorometer. Photosyn. Res. 10 (1), 51–62.
Smith, C.J., 2019. A geochemical investigation of the Monticchio Lakes, Monte Vulture, Basilicata, Italy. Thesis, Wesleyan University.
Spicciarelli, R., Marchetto, A., 2019. The contrasting evolution of two volcanic lakes lying in the same caldera (Monticchio, Mt Vulture, Italy) inferred from literature records. Adv. Oceanogr. Limnol. 10, 7949. https://doi.org/10.4081/aiol.2019.7949.
Stomp, M., Huisman, J., Vörös, L., et al., 2007. Colorful coexistence of red and green picocyanobacteria in lakes and seas. Ecol. Lett. 10, 290–298.
Tassi, F., Vaselli, O., Giannini, L., Tedesco, D., Nencetti, A., Montegrossi, G., Yalire, M.M., 2004. A low-cost and effective method to collect water and gas samples from stratified crater lakes: the 485 m deep lake Kivu (DRC). In: Proc. IAVCEI Gen. Ass., Puchon, Chile, pp. 14–19.
Tassi, F., Vaselli, O., Tedesco, D., Montegrossi, G., Darrah, T., Cuoco, E., Mapendano, M. Y., Poreda, R., Delgado Huertas, A., 2009. Water and gas chemistry at Lake Kivu (DRC): geochemical evidence of vertical and horizontal heterogeneities in a multi-basin structure. Geochem., Geophys., Geosyst. 10 https://doi.org/10.1029/2008GC002191.
Tassi, F., Rouwet, D., 2014. An overview of the structure, hazards, and methods of investigation of Nyos-type lakes from the geochemical perspective. J. Limnol. 73 (1), 39–54.
Tassi, F., Fazi, S., Rossetti, S., Pratesi, P., Ceccotti, M., Cabassi, J., et al., 2018a. The biogeochemical vertical structure renders a meromictic volcanic lake a trap for geogenic CO_2 (Lake Averno, Italy). PLoS ONE 13 (3), e0193914. https://doi.org/10.1371/journal.pone.0193914.
Tassi, F., Cabassi, J., Andrade, C., et al., 2018b. Mechanisms regulating CO_2 and CH_4 dynamics in the Azorean volcanic lakes (São Miguel Island, Portugal). J. Limnol. 77 (3), 483–504.
Tiodjio, R.E., Sakatoku, A., Nakamura, A., Tanaka, D., Fantong, W.Y., Tchakam, K.B., Ueda, A., 2014. Bacterial and archaeal communities in Lake Nyos (Cameroon, Central Africa). Sci. Rep. 4 (1), 1–10.
Tiodjio, R.E., Sakatoku, A., Fantong, W.Y., Tchakam, K.B., Tanyileke, G., Hell, V.J., Ueda, A., 2016. Vertical distribution of bacteria and archaea in a CO2-rich meromictic lake: a case study of Lake Monoun. Limnologica 60, 6–19.
R Core Team, 2018. R: a language and environment for statistical computing. In: Vienna, Austria.
Vaselli, O., Tassi, F., Montegrossi, G., Capaccioni, B., Giannini, L., 2006. Sampling and analysis of volcanic gases. Acta Vulcanol. 18, 65–76.
Venturi, S., Tassi, F., Cabassi, J., Randazzo, A., Lazzaroni, M., Capecchiacci, F., Vaselli, O., 2021. Exploring methane emission drivers in Wetlands: the cases of Massaciuccoli and Porta Lakes (Northern Tuscany, Italy). Appl. Sci. 11 (24), 12156.

Vergine, P., Amalfitano, S., Salerno, C., Berardi, G., Pollice, A., 2020. Reuse of ultrafiltered effluents for crop irrigation: on-site flow cytometry unveiled microbial removal patterns across a full-scale tertiary treatment. Sci. Total Environ. 718, 137298.
Vörös, L., Callieri, C., Balogh, K.V., Bertoni, R., 1998. Freshwater picocyanobacteria along a trophic gradient and light quality range. Phytoplankton and Trophic Gradients. Springer, Dordrecht, pp. 117–125.
Wang, K., Yan, H., Peng, X., et al., 2020. Community assembly of bacteria and archaea in coastal waters governed by contrasting mechanisms: a seasonal perspective. Mol. Ecol. 29 (19), 3762–3776.
Wang, B., Ma, B., Stirling, E., He, Z., Zhang, H., Yan, Q., 2023. Freshwater trophic status mediates microbial community assembly and interdomain network complexity. Environ. Pollut. 316, 120690.
Ward, C.S., Yung, C.M., Davis, K.M., et al., 2017. Annual community patterns are driven by seasonal switching between closely related marine bacteria. ISME J. 11 (6), 1412–1422.
Warnecke, F., Amann, R., Pernthaler, J., 2004. Actinobacterial 16S rRNA genes from freshwater habitats cluster in four distinct lineages. Environ. Microbiol. 6 (3), 242–253.
Whiticar, M.J., 1999. Carbon and hydrogen isotope systematics of bacterial formation and oxidation of methane. Chem. Geol. 161, 291–314.
Whitfield, M., 1978. Activity coefficients in natural waters. editor.. In: Pytkowicz, RM (Ed.), Activity Coefficients in Electrolyte Solutions. CRC Press, Boca Raton, Florida, pp. 153–300.
Wickham, H., 2009. ggplot2: Elegant Graphics for Data Analysis. Springer Science & Business Media.
Wickham, H., 2012. reshape2: flexibly reshape data: a reboot of the reshape package. R package version 1.2.
Wilhelm, E., Battino, R., Wilcock, R.J., 1977. Low-pressure solubility of gases in liquid water. Chem. Rev. 77 (2), 219–262.
Yu, S., He, R., Song, A., et al., 2019. Spatial and temporal dynamics of bacterioplankton community composition in a subtropical dammed karst river of southwestern China. Microbiologyopen 8 (9), e00849.
Zakaria, B.S., Lin, L., Dhar, B.R., 2019. Shift of biofilm and suspended bacterial communities with changes in anode potential in a microbial electrolysis cell treating primary sludge. Sci. Total Environ. 689, 691–699.
Zimmer, M., Tassi, F., Vaselli, O., Kujawa, C., Cabassi, J., Erzinger, J., 2016. The gas membrane sensor (GMS) method: a new analytical approach for real-time gas concentration measurements in volcanic lakes. Geol. Soc., London, Special Public. 437 (1), 223–232.